Research Square

Preprints are preliminary reports that have not undergone peer review.
They should not be considered conclusive, used to inform clinical practice,
or referenced by the media as validated information.

# Formulation, Dispersion Characterization, and In Vitro Release of Meloxicam-Loaded Nanoemulgels

**Abhijit Merekar**

anmerekar@yahoo.co.in

Dr. Vitthalrao Vikhe Patil Foundation's College of Pharmacy,

**Smita Merekar**

Dr. Vitthalrao Vikhe Patil Foundation's College of Pharmacy,

**Pratiksha Unhale**

Dr. Vitthalrao Vikhe Patil Foundation's College of Pharmacy,

**Manisha Tayde**

Shree Panchavati Education Society's Nasik. Smt.Narmadaben Popatlal Thakkar Institute of Pharmacy

**Prasad Patrekar**

Eklavya College of Pharmacy,

**Manish Bhise**

Vidyaniketan College of Pharmacy

**Research Article**

**Keywords:** meloxicam, nanoemulgel, colloidal dispersion, in vitro release, particle size

**Posted Date:** November 3rd, 2026

**DOI:** https://doi.org/10.21203/rs.3.rs-10981515/v1

**License:** This work is licensed under a Creative Commons Attribution 4.0 International License.
Read Full License

**Additional Declarations:** No competing interests reported.

# Formulation, Dispersion Characterization, and In Vitro Release of Meloxicam-Loaded Nanoemulgels

Abhijit Merekar1*, Smita Merekar², Pratiksha Unhale3, Manisha Tayde4, Prasad Patrekar 5, Manish Bhise 6

1 Professor, Department of Pharmaceutics, Dr. Vitthalrao Vikhe Patil Foundation's College of Pharmacy, Vilad Ghat, Ahilyanagar, Maharashtra, India 414111.2. Associate Professor, Department of Pharmaceutical Chemistry, Dr. Vithalrao Vikhe Patil Foundation's College of Pharmacy, Vilad Ghat, Ahilyanagar, Maharashtra, India – 414111

3. Department of Pharmaceutics, Dr. Vitthalrao Vikhe Patil Foundation's College of Pharmacy, Vilad Ghat, Ahilyanagar, Maharashtra, India 414111. Affiliated to Savitribai Phule Pune University, Pune.India

4. Department of Pharmaceutical Chemistry, Shree Panchavati Education Society, Nashik. Smt.Narmadaben Popatlal Thakkar Institute of Pharmacy, Nashik, Maharashtra 422003, India

5. Associate Professor, Department of Pharmaceutics, Eklavya College of Pharmacy, Tasgaon, Manerajuri Road, Vasumbe. Tal-Tasgaon, Dist-Sangli. 416312, India

6. Professor, Vidyaniketan College of Pharmacy, Anjangaon Surji Dist . Amaravati 444705, India

Corresponding Author: Abhijit N. Merekar, India
Contact no: 9665501129
Email ID anmerekar@yahoo.co.in

**Abstract**

Meloxicam-loaded nanoemulgels were prepared using selected oils, Tween 80, PEG 400, and Carbopol 934 and evaluated for dispersion and topical performance. We compared nine formulations for appearance, pH, drug content, viscosity, and release across a dialysis membrane. The lead formulation produced 96.91% release at 60 min and showed a mean droplet size of 118.5 nm, polydispersity index of 0.440, and zeta potential of −28 mV. Infrared spectra retained the principal meloxicam bands. The findings demonstrate formulation feasibility, while skin permeation, validated stability, and biological performance require further investigation.

Keywords: meloxicam; nanoemulgel; colloidal dispersion; in vitro release; particle size

## 1. Introduction

Rheumatoid arthritis (RA) is a systemic immune-mediated disease in which persistent synovial inflammation promotes pain, morning stiffness, cartilage loss and progressive structural damage. It affects peripheral joints symmetrically and may also produce fatigue, cardiovascular complications and loss of functional independence. Contemporary reviews emphasize early diagnosis, treat-to-target monitoring and prompt use of disease-modifying antirheumatic drugs [1] [2] [3] [4]. Current treatment guidance distinguishes control of the underlying immune process from short-term symptomatic relief [5] [6]. Genetic susceptibility, environmental exposure and immune-cell dysregulation contribute to disease heterogeneity [7] [8]. Non-steroidal anti-inflammatory drugs (NSAIDs) therefore remain adjuncts for pain and inflammation rather than disease-modifying treatment. Because many patients require prolonged symptom management, route of administration, local tolerability and adherence are relevant formulation considerations.

Meloxicam is an oxicam NSAID used in painful inflammatory disorders. Its preferential inhibition of cyclooxygenase-2 reduces prostaglandin synthesis, although it retains class-related NSAID precautions. Low aqueous solubility can complicate dissolution, uniform incorporation and release from conventional aqueous gels. Recent research has examined long-acting meloxicam delivery (9), liposome and microemulsion systems (10), ethosomal hydrogels (11), microneedle-based delivery (12), deformable liposomal hydrogels (13), hydrogel-based solid dispersions (14) and flavosome carriers (15). Together, these reports support the feasibility of dispersed or vesicular carriers while also showing that dermal or transdermal claims require direct skin-transport evidence.

For a poorly water-soluble molecule, a successful topical vehicle must maintain the drug in a solubilized or finely dispersed state during manufacture, storage and application. Precipitation can reduce the drug available for diffusion, whereas excessive affinity for the internal oil phase may retard partitioning into the aqueous receptor or skin. Formulation development must therefore balance solubilization capacity with release from the carrier. The oil phase, surfactant-to-cosurfactant ratio, aqueous fraction and polymer concentration are interdependent variables rather than isolated ingredients.

Topical application offers convenient administration and the possibility of localized exposure, but the stratum corneum is a highly effective diffusional barrier. A formulation described as “topical” cannot automatically be considered “transdermal”: the latter requires evidence that drug crosses the skin into or toward systemic circulation. Nanoemulsions may improve apparent solubilization of lipophilic drugs and provide a large interfacial area. Nevertheless, their low viscosity may cause runoff and short residence time. Converting a nanoemulsion into a nanoemulgel by incorporating it into a polymeric matrix can improve handling, spreadability and contact with the application site. Recent work has demonstrated this platform with anti-inflammatory and osteoarthritis-oriented systems (16) (17), topical antimicrobials (18), aceclofenac (19), desonide (20), combination antipsoriatic therapy (21), crisaborole (22) and minocycline (23).

A nanoemulgel contains an oil-in-water or water-in-oil nanodispersion immobilized within a three-dimensional gel network. The dispersed droplets act as drug reservoirs, surfactants lower interfacial tension, cosurfactants improve interfacial flexibility, and the hydrated polymer provides viscosity. Carbopol 934 is widely used because neutralization causes polymer-chain expansion and development of a clear gel. Tween 80 is a non-ionic surfactant with broad pharmaceutical use, while PEG 400 can

function as a cosolvent and cosurfactant. The combination may facilitate formation of a small-droplet dispersion, but excessive surfactant can affect skin tolerability and must be justified by performance.

The versatility of nanoemulgels is illustrated by systems developed for thymoquinone, atorvastatin, antibacterial thiazole derivatives, terbinafine, 5-fluorouracil, curcumin, mupirocin, andrographolide, lornoxicam, statins, desonide and other poorly soluble agents (18–37). Across these studies, evaluation commonly combines appearance, pH, assay, rheology, droplet-size distribution, zeta potential, release and, when justified, ex vivo or in vivo performance. This evidence base also demonstrates why a nanoscale mean diameter or rapid membrane release alone cannot establish enhanced clinical efficacy.

Critical quality attributes for a topical nanoemulgel include physical homogeneity, absence of phase separation, acceptable pH, assay uniformity, rheological behaviour compatible with application, droplet-size distribution and reproducible drug release. Mean droplet size must be interpreted together with polydispersity index (PDI), because a nanoscale mean can coexist with a broad population. Zeta potential provides information about electrostatic repulsion, but formulations stabilized with non-ionic surfactants may also depend strongly on steric stabilization. Neither measurement alone replaces storage-stability testing.

Diffusion-cell results require particularly careful terminology. A synthetic dialysis membrane mainly retains formulation while allowing dissolved drug to enter the receptor phase; it is useful for comparative in vitro release testing but does not reproduce the barrier properties of skin. Current semisolid testing literature emphasizes apparatus qualification, controlled temperature and stirring, defined membrane and diffusion area, sink conditions, sampling correction, discriminatory ability and appropriate statistical treatment (38) (39) (40) . Accordingly, the present outcome is described as in vitro release, not skin permeation or transdermal flux.

Against this background, the present study prepared nine meloxicam nanoemulgels using castor, oleic or olive oil with Tween 80, PEG 400 and Carbopol 934. The formulations were compared using the experimental observations available in the source record. The manuscript deliberately avoids pharmacological, clinical, bioavailability and long-term-stability claims that were not supported by corresponding experimental data.

The scientific rationale was that the selected oils could provide a lipophilic domain for meloxicam, Tween 80 and PEG 400 could support dispersion formation, and Carbopol 934 could convert the fluid system into an application-friendly semisolid. The work therefore addressed three linked questions: whether visually stable nanoemulsion regions could be identified, whether the resulting gels possessed acceptable physicochemical attributes, and whether their comparative release profiles could identify a lead formulation for more rigorous future evaluation.

**Study objective**

The objective was to prepare nine meloxicam nanoemulgels using three candidate oils and to identify a formulation with suitable appearance, skin-compatible pH, drug content, viscosity and release behaviour for further development.

## 2. Materials and Methods

### 2.1 Materials

Meloxicam was obtained from Demtech Pharma (Mumbai, India). Oleic acid, olive oil, castor oil, PEG 400, Carbopol 934, methyl paraben and propyl paraben were procured from Modern Industries (India). Tween 80 and triethanolamine were obtained from Chemsworth Chemicals (India). Other reagents were of analytical grade, and distilled water was used throughout.

The three oils were investigated as alternative internal phases. Tween 80 was selected as the principal non-ionic surfactant, PEG 400 as cosurfactant/cosolvent, Carbopol 934 as the gel-forming polymer and triethanolamine as the neutralizing agent. Methyl paraben and propyl paraben were included as preservatives, while rose oil was added in a quantity sufficient to improve organoleptic acceptability. Materials were used as received. Supplier batch numbers and certificates of analysis were not included in the available study record and should be retained with the underlying laboratory documentation.

#### 2.1.1 Overall experimental workflow

The investigation followed a sequential workflow: preliminary excipient screening; aqueous-titration mapping of candidate nanoemulsion regions; preparation of nine meloxicam compositions; incorporation into hydrated Carbopol gel; physicochemical evaluation; comparative in vitro release testing; and particle-size, PDI, zeta-potential and FTIR examination of the lead formulation. Each batch was coded F1–F9 to maintain traceability between composition and evaluation records.

#### 2.1.2 Basis of excipient selection

The source investigation screened meloxicam against candidate oils and selected the working oil phases on the basis of drug accommodation and emulsification behaviour. Surfactant and cosurfactant selection considered visual dispersibility and compatibility with an aqueous gel. Complete equilibrium-solubility values were not supplied; therefore, no unverified values are introduced. Reproducible confirmation would require addition of excess drug to each vehicle, controlled equilibration, separation of undissolved material and assay of the clear supernatant.

### 2.2 Preliminary nanoemulsion region screening

Oil, Tween 80 and PEG 400 were screened using aqueous titration. Surfactant-to-cosurfactant mixtures were evaluated at ratios of 1:1, 1:2 and 2:1. Oil and surfactant mixture were blended, and distilled water was added gradually until turbidity appeared. Clear, isotropic, low-viscosity systems were recorded as the nanoemulsion region. The diagrams were used as preliminary composition maps rather than as proof of thermodynamic stability.

For each surfactant-to-cosurfactant ratio, the components were mixed thoroughly before titration. Water was introduced in small increments with mixing, and the visual state was recorded after equilibration. The proportions corresponding to clear systems were plotted on triangular coordinates. Visual mapping was used only to define a workable composition region; polarized-light microscopy, conductivity testing and free-energy measurements were not available to establish microstructural identity.

At each titration point, component percentage can be expressed as the mass of the component divided by the total mass of oil, Smix and water, multiplied by 100. Points remaining clear and free from visible separation were used to outline the candidate region, whereas turbid, phase-separated or excessively

viscous systems were excluded. Since clarity is an operational observation, these diagrams were treated as formulation guides and not as conclusive proof of thermodynamic stability.

### 2.3 Preparation of nanoemulsion and nanoemulgel

Meloxicam was dispersed in the designated oil phase. Tween 80 and PEG 400 were premixed and incorporated under magnetic stirring, followed by dropwise addition of water. Carbopol 934 was separately hydrated in distilled water and neutralized with triethanolamine. The nanoemulsion was then incorporated gradually into the gel base until a visually homogeneous product was obtained.

During incorporation, mixing was continued at a controlled practical rate to minimize local polymer aggregation and entrapped air. Preservatives and rose oil were included as reported in the source formulation record. Prepared batches were transferred to closed containers and retained for evaluation. Exact homogenization speed, sonication energy, processing duration and final batch mass were not present in the supplied record; these parameters were not available for analysis and remain limitations for droplet-size reproducibility and scale-up.

#### 2.3.1 Preparation of Carbopol gel base

The required Carbopol 934 was sprinkled gradually over distilled water with gentle stirring to avoid dry polymer agglomerates. The dispersion was allowed to hydrate until uniform and was then neutralized carefully with triethanolamine to develop gel consistency. Excessive agitation was avoided because entrapped air can interfere with appearance, viscosity measurement, filling and dose uniformity.

#### 2.3.2 Incorporation and finishing

The nanoemulsion was incorporated into the gel base in portions. Each portion was mixed to visual uniformity before the next was added. Preservatives and fragrance were distributed throughout the batch, after which the product was allowed to stand to reduce entrapped air. Finished nanoemulgels were transferred to clean, closed containers labelled with formulation code and preparation date.

### 2.4 Experimental design statement

Nine formulations were compared empirically. Because the reported compositions change oil identity and oil amount without a fully documented randomized factorial design or replicate-level model data, inferential design-of-experiments statistics were not retained. Results are therefore presented descriptively.

F3 was treated as the lead batch because it showed the highest observed 60-min release in the reported data set and was associated with the supplied particle-size and zeta-potential records. This selection criterion is empirical and does not imply statistically demonstrated superiority.

### 2.5 Formulation composition

| Batch | Meloxicam | Oil | Oil amount | Tween 80 | PEG 400 | Carbopol 934 |
|---|---|---|---|---|---|---|
| F1 | 15 | Castor oil | 6.3 | 11.1 | 5.3 | 250* |
| F2 | 15 | Castor oil | 9.4 | 11.1 | 5.3 | 250* |
| F3 | 15 | Castor oil | 14.5 | 11.1 | 5.3 | 250* |
| F4 | 15 | Oleic acid | 6.6 | 11.1 | 5.3 | 250* |
| F5 | 15 | Oleic acid | 9.9 | 11.1 | 5.3 | 250* |
| F6 | 15 | Oleic acid | 14.3 | 11.1 | 5.3 | 250* |
| F7 | 15 | Olive oil | 6.7 | 11.1 | 5.3 | 250* |

| Batch | Meloxicam | Oil | Oil amount | Tween 80 | PEG 400 | Carbopol 934 |
|---|---|---|---|---|---|---|
| F8 | 15 | Olive oil | 10.1 | 11.1 | 5.3 | 250* |
| F9 | 15 | Olive oil | 14.7 | 11.1 | 5.3 | 250* |

***Table 1. Reported composition of meloxicam nanoemulgels (amounts as supplied in the source record). *The source table reports 75 for F2 and 250 for other batches; units and final batch size should be confirmed before submission.***

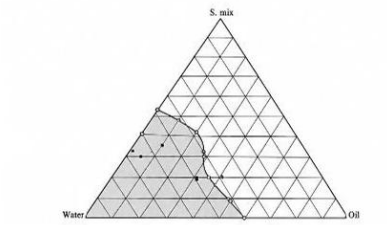



***Figure 1A. Preliminary pseudo-ternary diagram at Smix 1:1.***

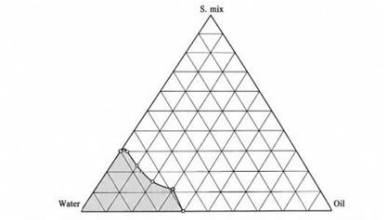



***Figure 1B. Preliminary pseudo-ternary diagram at Smix 1:2.***

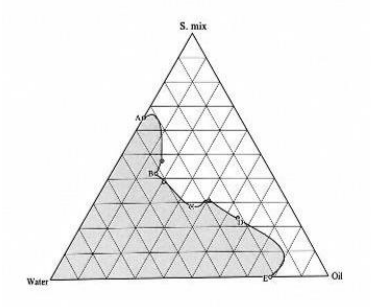



***Figure 1C. Preliminary pseudo-ternary diagram at Smix 2:1.***

### 2.6 Evaluation procedures

#### 2.6.1 Appearance, homogeneity and pH

Colour, consistency, grittiness, phase separation and homogeneity were assessed visually. For pH measurement, 1 g of formulation was dispersed in 100 mL distilled water, equilibrated for 2 h and measured in triplicate using a calibrated digital pH meter.

The electrode was rinsed between measurements, and the mean of three readings was reported. The visual examination was performed against a contrasting background under ambient laboratory illumination. Because no validated numerical scoring system was used, appearance and homogeneity findings are reported qualitatively.

For the thin-film homogeneity check, a small amount of formulation was spread between clean glass surfaces and examined for coarse particles, lumps and oil droplets. Visible syneresis, oiling-out or

separation was recorded as physical instability. The pH dispersion procedure was kept the same for all batches to minimize matrix-related differences between measurements.

### 2.6.2 Drug content

One gram of nanoemulgel was dispersed in phosphate buffer (pH 7.4), diluted appropriately and analyzed by UV spectrophotometry. Meloxicam was quantified at 361 nm using the calibration equation $y = 0.0177x + 0.0607$ over 5–25 µg/mL (reported $R^2 = 0.9998$).

The blank contained the corresponding vehicle/solvent system. Concentrations were calculated from the regression equation after bringing absorbance within the calibration range. The source record documented linearity only; selectivity against excipients, recovery, repeatability, intermediate precision, robustness, detection limit and quantification limit were not sufficiently documented to claim full analytical-method validation.

Drug content (%) was calculated as the measured quantity of meloxicam divided by the theoretical quantity and multiplied by 100, after applying all dilution factors. Extraction time, extraction solvent, filtration procedure, the number of independently prepared samples and batch-level variability were not documented in the available record. These details are particularly important for a lipophilic drug because incomplete extraction from the oil–polymer matrix can produce an apparent low assay.

### 2.6.3 Viscosity and spreadability

Viscosity was measured using a Brookfield viscometer with spindle 64 at 10, 20 and 30 rpm. The reported batch values are presented in Table 2. Spreadability was assessed by the slide method; numerical spreadability records were not available and therefore no quantitative claim is made.

Measurements were performed after allowing the sample to equilibrate at the measurement condition. Because the supplied summary contained one viscosity value per formulation but no shear-rate-specific replicate table, the values are used for batch comparison only. Extrudability was assessed operationally from the mass of gel expelled from a collapsible tube under the reported load; complete numerical records were unavailable.

Spindle immersion depth and sample volume were maintained consistently, and readings were taken after rotational stabilization. Ideally, viscosity should be reported at every rotational speed with temperature, torque range and replicate variability. The available single batch values are therefore treated as comparative apparent viscosities rather than a complete rheological characterization.

#### 2.6.3.1 Spreadability and extrudability

Spreadability was assessed using the glass-slide method. A defined quantity of gel was placed between two slides, a standard mass was applied to form a uniform film, and the time required for the upper slide to travel a defined distance was observed. Spreadability may be expressed as $S = M \times L/t$, where M is the applied mass, L is distance travelled and t is separation time. Extrudability was evaluated from the quantity of gel expelled as a continuous ribbon from a collapsible tube under the specified load. Since complete batch-wise numerical records were unavailable, these observations were not used for quantitative ranking.

### 2.6.4 In vitro release

A dialysis membrane was hydrated in phosphate buffer (pH 7.4) for 24 h and mounted on a modified Franz diffusion cell with a 50 mL receptor compartment. Nanoemulgel (1 g) was applied to the membrane. The receptor was maintained at 37 ± 1 °C and stirred at 50 rpm. At specified times, 1 mL

was withdrawn and replaced with fresh medium. Samples were measured at 361 nm. The outcome is correctly described as release across a synthetic membrane, not ex vivo skin permeation.

Sampling was conducted at 5, 10, 15, 20, 30, 45, 50 and 60 min. Replacement with an equal volume of fresh medium was intended to maintain receptor volume and sink conditions. Cumulative release values were taken from the supplied record. Membrane molecular-weight cut-off, effective diffusion area, receiver-volume correction formula and replicate variability were not reported; consequently, flux and permeability coefficients were not calculated. This distinction follows current emphasis on controlled diffusion-cell methodology for semisolid products (38) (39) (40) .

Before assembly, the receptor compartment was checked for absence of trapped air beneath the membrane. The receptor was stirred continuously to reduce formation of an unstirred boundary layer, and withdrawn samples were replaced immediately with fresh medium. For serial sampling, corrected cumulative mass should include the drug remaining in the receptor plus the mass removed in all earlier aliquots. The source values were retained as reported because the original absorbance and sampling-correction worksheet was unavailable.

### 2.6.5 Particle size, PDI, zeta potential and FTIR

The selected formulation was analyzed for hydrodynamic size, polydispersity index and zeta potential. FTIR spectra of meloxicam and drug–oil mixtures were compared qualitatively for retention or marked displacement of characteristic bands. Instrument settings and replicate details were not available in the source record and should be added if available.

Particle-size and electrokinetic-potential outputs were interpreted directly from the supplied instrument plots. The PDI was used as an indicator of breadth of the size distribution. FTIR interpretation was limited to qualitative comparison; the spectra were not used to infer accelerated or long-term stability.

For light-scattering analysis, the formulation should be diluted with a compatible filtered dispersant only to the extent required to avoid multiple scattering. The cuvette must be free from dust and bubbles. Reporting should include dispersant viscosity and refractive index, measurement temperature, equilibration time, scattering configuration and number of runs. Zeta potential should similarly state dispersant conductivity and the conversion model used by the instrument.

For FTIR compatibility assessment, spectra of the pure drug and corresponding drug–excipient mixtures were compared across the recorded wavenumber range. Retention of the principal fingerprint pattern was used as an initial compatibility indication. Small intensity differences were not treated as evidence of chemical interaction because they can result from dilution, baseline correction, sample contact and overlap with excipient bands.

### 2.6.6 Data handling

Results with documented batch-level values are presented descriptively. No inferential statistical comparison was performed because replicate-level data, randomization details and a complete prespecified experimental design were unavailable. Conflicting regression outputs from the preliminary kinetic analysis were excluded rather than reconciled by assumption. Numerical values were rounded consistently with the source tables.

## 3. Results and Discussion

### 3.1 UV spectrophotometric response

Meloxicam showed an absorption maximum at 361 nm in phosphate buffer (pH 7.4). The reported response was linear from 5 to 25 µg/mL with regression equation $y = 0.0177x + 0.0607$ and $R^2 = 0.9998$. These data support routine quantification for the formulation study; they do not constitute a complete validation because accuracy, precision, specificity, robustness and detection limits were not documented.

The selected wavelength is consistent with the visible long-wavelength absorption feature shown in the supplied spectrum. The small intercept relative to the working absorbance range and the high coefficient of determination indicate proportional response within the tested interval. However, $R^2$ alone is not a validation criterion. Matrix-matched recovery and precision data would be required to confirm that oil, surfactant, cosurfactant and polymer do not bias quantification.

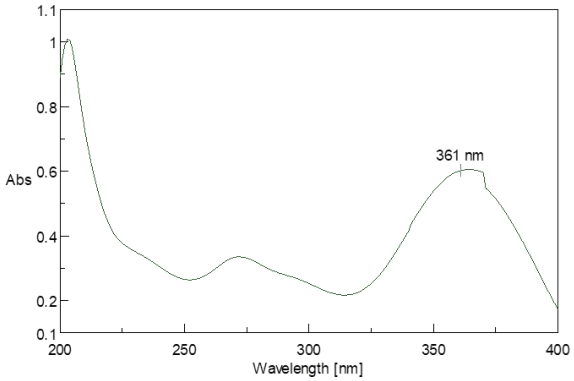



***Figure 2A. Reported UV absorption spectrum of meloxicam in phosphate buffer (pH 7.4).***

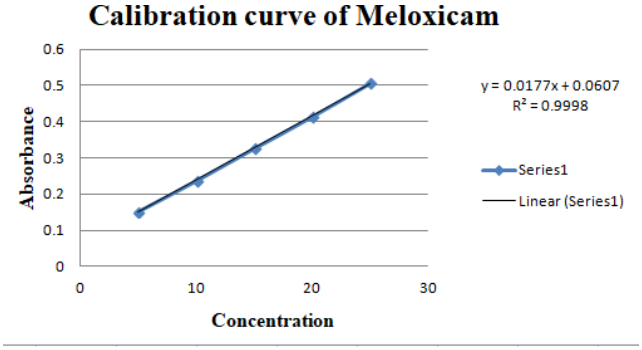



***Figure 2B. Reported calibration curve of meloxicam (5–25 µg/mL).***

### 3.2 FTIR compatibility assessment

The spectra retained the principal meloxicam bands in the examined drug–oil mixtures. No prominent new band was evident in the supplied spectra. This qualitative observation suggests no readily detectable chemical interaction under the measurement conditions, but it should not be interpreted as proof of long-term compatibility.

Minor changes in intensity or band shape can arise from dilution, sample contact and overlap with excipient signals. Therefore, the preserved fingerprint pattern is reported conservatively as compatibility screening. Confirmation would benefit from a tabulated peak assignment and complementary thermal or solid-state analysis when original experimental outputs are available.

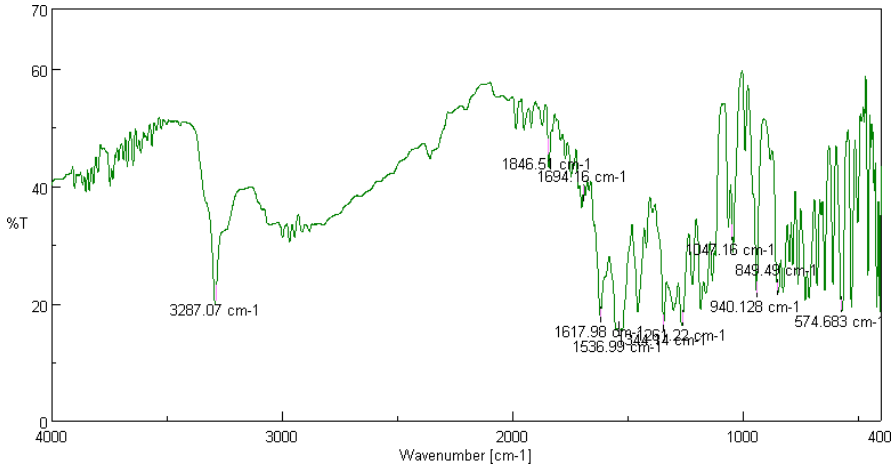



***Figure 3A. FTIR spectrum of meloxicam.***

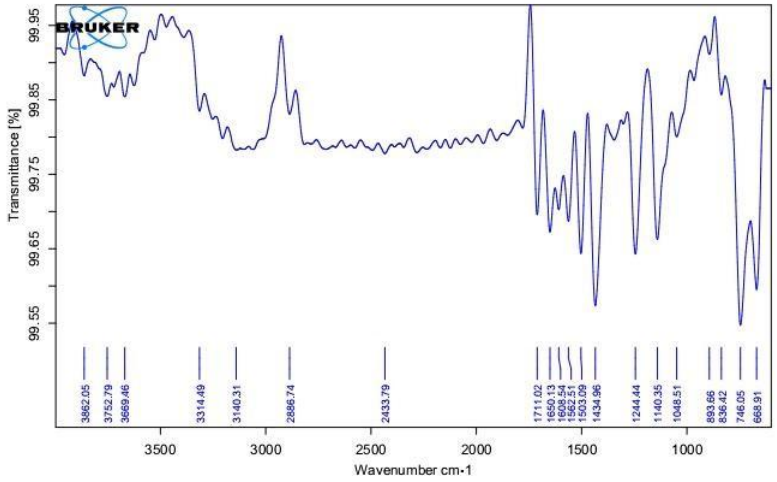



***Figure 3B. FTIR spectrum of meloxicam in castor oil.***

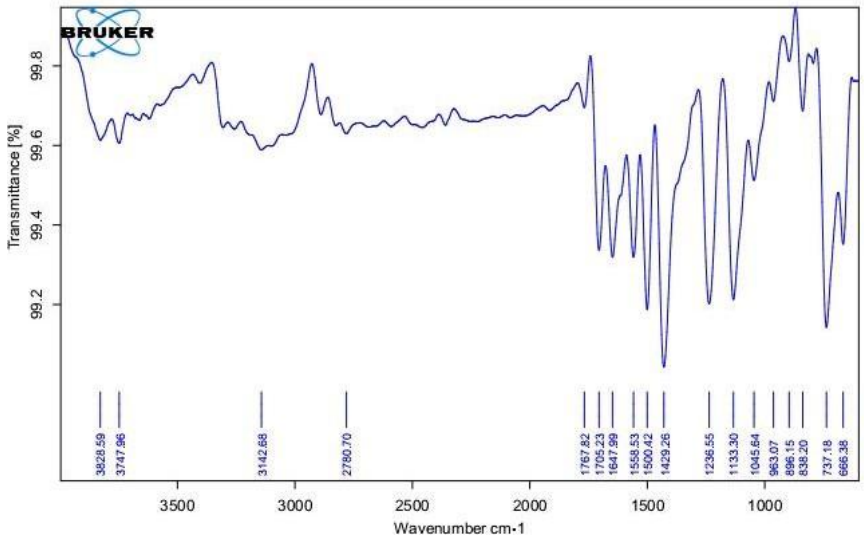



***Figure 3C. FTIR spectrum of meloxicam in oleic acid.***

The spectra are presented as supplied. Peak assignments and acquisition parameters (instrument, scan range, resolution and number of scans) were unavailable; the spectra are therefore interpreted only as qualitative compatibility screening.

### 3.3 Physical characteristics and viscosity

All batches were reported to be smooth and homogeneous without visible phase separation. The pH range of 5.6–6.4 is compatible with topical use, although irritation cannot be inferred without a validated irritation test. Drug content ranged from 90.36% to 99.40%; batch-level replicate values and variability were not supplied and should be retained in laboratory records.

The absence of visible separation immediately after preparation indicates successful macroscopic incorporation of the dispersed phase into the gel network. The pH values fall within a generally acceptable range for cutaneous semisolids and are unlikely to create marked discomfort solely because of acidity or alkalinity. Nevertheless, formulation pH does not replace irritation or sensitization testing. The spread in drug-content values suggests that mixing and extraction efficiency should be examined, particularly for batches near 90%.

| Formulation | Viscosity (cP) |
|---|---|
| F1 | 3900 |
| F2 | 6759 |
| F3 | 4976 |
| F4 | 8523 |
| F5 | 5294 |
| F6 | 7653 |
| F7 | 6205 |
| F8 | 5921 |
| F9 | 7623 |

***Table 2. Reported viscosity of meloxicam nanoemulgel formulations.***

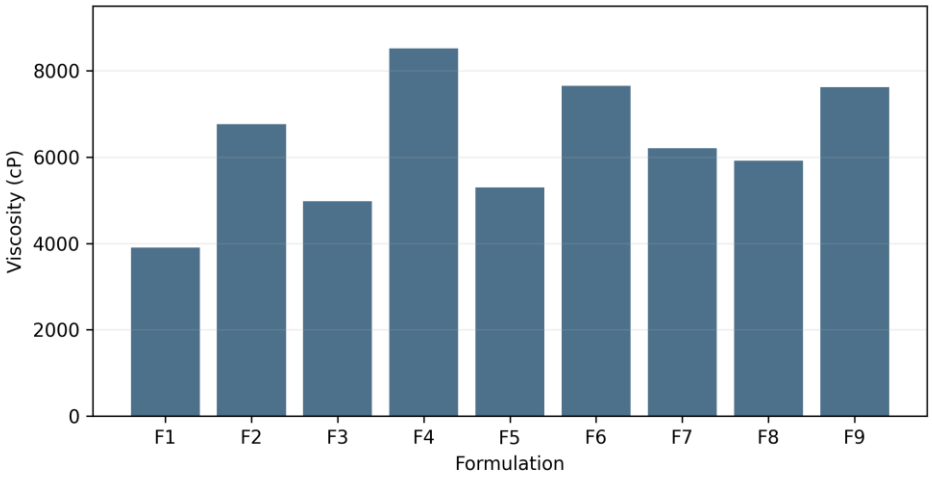



***Figure 4. Comparative viscosity of formulations F1–F9.***

Viscosity varied approximately 2.2-fold across the batches. Because oil identity, oil amount and the reported Carbopol amount were not controlled as a single complete factorial design, the values should not be used to attribute causality to one ingredient. Rheograms and replicate measurements would strengthen the assessment.

F4 gave the highest reported viscosity (8523 cP), whereas F1 gave the lowest (3900 cP). F3, the lead release batch, showed an intermediate viscosity of 4976 cP. This combination may have allowed easier diffusion than in the most viscous systems while maintaining a gel-like consistency. That explanation remains a formulation hypothesis because shear stress–shear rate curves, yield stress, thixotropic

recovery and statistical association with release were not available. Comparable topical nanoemulgel studies similarly treat rheology as a critical performance attribute because it affects handling, residence and diffusion (16–31).

### 3.4 In vitro release

| Time | F1 | F2 | F3 | F4 | F5 | F6 | F7 | F8 | F9 |
|---|---|---|---|---|---|---|---|---|---|
| 5 | 5.07 | 6.38 | 8.15 | 5.12 | 6.72 | 7.43 | 7.98 | 5.12 | 6.32 |
| 10 | 12.41 | 13.35 | 15.03 | 11.45 | 11.85 | 12.91 | 12.65 | 11.65 | 9.12 |
| 15 | 25.97 | 26.72 | 28.14 | 23.55 | 25.92 | 24.1 | 26.98 | 23.64 | 21.43 |
| 20 | 36.15 | 39.42 | 41.21 | 37.02 | 34.97 | 39.68 | 39.86 | 38.32 | 36.54 |
| 30 | 47.32 | 49.08 | 52.37 | 47.11 | 46.29 | 51.64 | 50.37 | 45.33 | 49.21 |
| 45 | 63.98 | 69.23 | 71.45 | 61.34 | 60.12 | 69.34 | 69.74 | 64.34 | 68.43 |
| 50 | 74.32 | 77.47 | 80.09 | 73.11 | 71.12 | 76.12 | 79.43 | 72.65 | 75.86 |
| 60 | 87.32 | 92.45 | 96.91 | 94.11 | 90.12 | 91.23 | 95.01 | 82.08 | 85.23 |

***Table 3. Cumulative meloxicam release (%) across a dialysis membrane.***

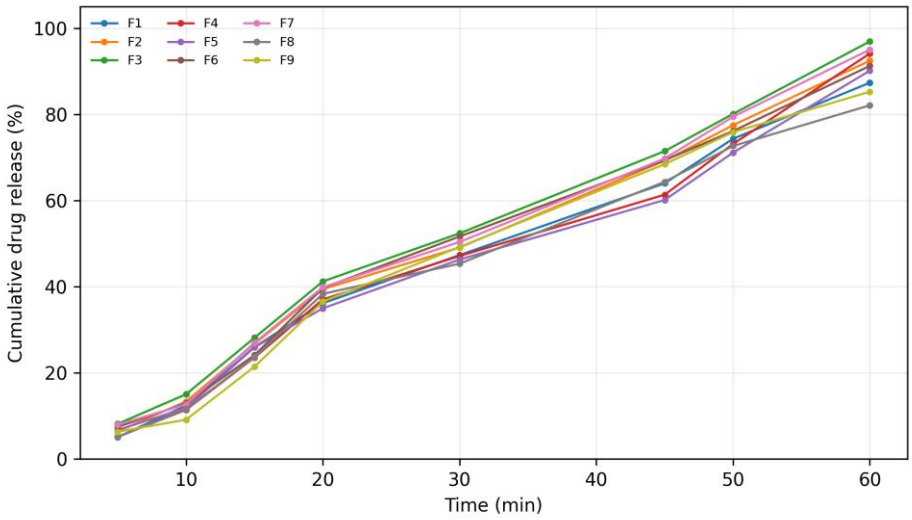



***Figure 5. In vitro release profiles of formulations F1–F9.***

Release increased with time for every batch. At 60 min, the observed values ranged from 82.08% (F8) to 96.91% (F3). F3 therefore showed the highest endpoint release in this data set, closely followed by F7 (95.01%) and F4 (94.11%). Without replicate-level variability and prespecified statistical comparisons, these differences should be interpreted descriptively.

The curves showed no abrupt decline, supporting internally consistent accumulation over the sampling interval. Differences between batches became more evident after approximately 30 min. Oil identity, oil level, drug partitioning between the dispersed phase and receiver, and gel viscosity may all contribute to these profiles. Because multiple variables changed simultaneously, the present data cannot isolate the effect of an individual component. The rapid endpoint release also means that “sustained release” is not an appropriate description for this 60-min data set.

The dialysis membrane primarily separates formulation from receptor and provides little resemblance to the organized lipid–protein barrier of the stratum corneum. Accordingly, the present experiment demonstrates drug liberation and diffusion under the specified conditions, not dermal deposition or transdermal delivery. A follow-up study should use validated human or porcine skin, report donor dose

and diffusion area, verify sink conditions, quantify retained drug in skin layers and calculate steady-state flux with uncertainty (38–40).

### 3.5 Particle size and electrokinetic potential

The characterized formulation showed a mean diameter of 118.5 nm and PDI of 0.440. The nanoscale mean supports classification as a nanodispersion, whereas the PDI indicates a moderately broad distribution rather than a highly monodisperse system. The reported zeta potential was −28 mV, suggesting an electrostatic contribution to dispersion stability. Long-term stability nevertheless requires direct assessment.

The PDI deserves particular attention: a value of 0.440 suggests meaningful heterogeneity and may indicate that homogenization or sonication conditions require refinement. The negative zeta potential is compatible with repulsive stabilization, but non-ionic Tween 80 can also provide steric stabilization; therefore, a single zeta-potential measurement should not be used as a stand-alone predictor of shelf life. Recent nanoemulsion and nanoemulgel investigations generally combine size, PDI and surface charge with centrifugation, thermal cycling and storage-time measurements (16–37).

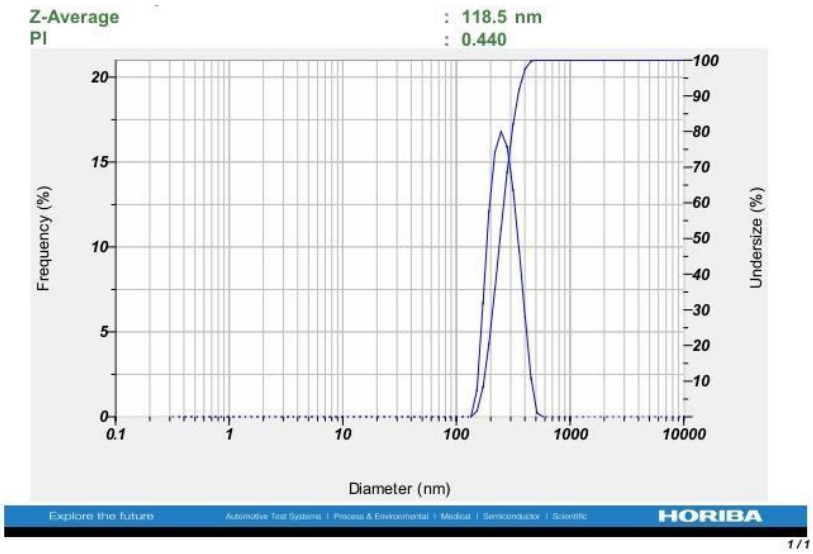



*Figure 6. Particle-size distribution of the characterized meloxicam nanoemulgel (mean 118.5 nm; PDI 0.440).*

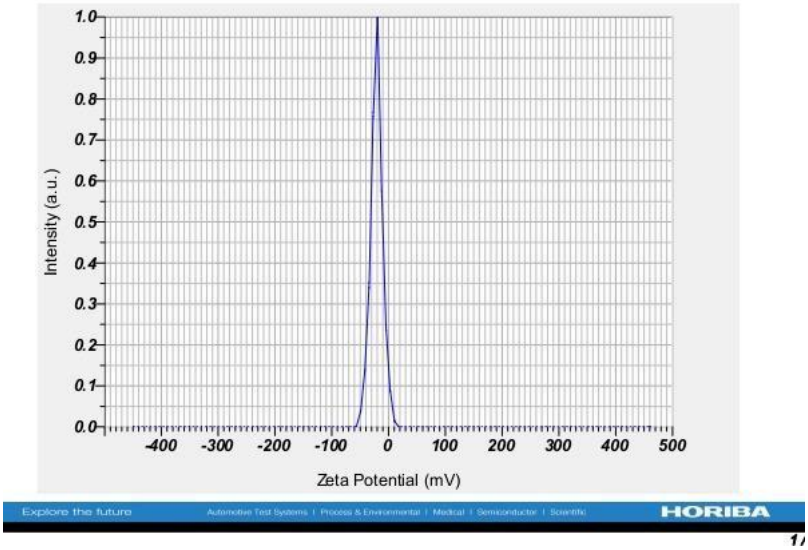



***Figure 7. Zeta-potential distribution of the characterized meloxicam nanoemulgel (−28 mV).***

The preliminary manuscript contained mutually inconsistent Higuchi regression coefficients in its table and plotted figure. Because the underlying transformed data and replicate records were unavailable, the kinetic-model result was removed rather than selecting one of the conflicting values.

### 3.6 Study limitations

This study is limited by the absence of replicate-level raw data for several outcomes, incomplete analytical validation and instrument details, no ex vivo skin model, no validated stability protocol, and no pharmacological comparison. The composition table also requires confirmation of units, final batch size and the reported Carbopol value for F2. Consequently, the findings support formulation feasibility only; they do not establish transdermal delivery, bioavailability enhancement, anti-inflammatory efficacy, analgesic efficacy or reduced gastrointestinal toxicity.

## 4. Conclusion

Meloxicam nanoemulsions with acceptable visual characteristics and topical pH were prepared. F3 produced the highest recorded 60-min in vitro release (96.91%) and the characterized formulation showed a mean size of 118.5 nm, PDI 0.440 and zeta potential −28 mV. These results justify further development using confirmed batch compositions, replicate testing, validated analytical procedures, ex vivo skin permeation, stability testing and appropriate biological evaluation.

## Declarations

Acknowledgement: The authors thank Dr. Vitthalrao Vikhe Patil Foundation’s College of Pharmacy, Ahilyanagar, for facilities and academic support.

Conflict of interest: None declared. Funding: No external funding was reported. Ethics approval: Not applicable.

**Data Availability Statement:** The datasets generated during and/or analysed during the current study are available from the corresponding author on reasonable request.

## References


1. Radu, A.F.; Bungau, S.G. Management of Rheumatoid Arthritis: An Overview. Cells 2021, 10(10), 2857. https://doi.org/10.3390/cells10112857.
2. Cush, J.J. Rheumatoid Arthritis: Early Diagnosis and Treatment. Rheum Dis Clin North Am 2022, 48(2), 537-547. https://doi.org/10.1016/j.rdc.2022.02.010.
3. Smolen, J.S.; Aletaha, D.; Barton, A.; Burmester, G.R.; Emery, P.; Firestein, G.S.; et al. Rheumatoid arthritis. Nat Rev Dis Primers 2018, 4, 18001. https://doi.org/10.1038/nrdp.2018.1.
4. Gao, Y.; Zhang, Y.; Liu, X. Rheumatoid arthritis: pathogenesis and therapeutic advances. MedComm (2020) 2024, 5(3), e509. https://doi.org/10.1002/mco2.509.
5. Singh, J.A. Treatment Guidelines in Rheumatoid Arthritis. Rheum Dis Clin North Am 2022, 48(3), 679-689. https://doi.org/10.1016/j.rdc.2022.03.005.
6. Venetsanopoulou, A.I.; Alamanos, Y.; Voulgari, P.V.; Drosos, A.A. Epidemiology of rheumatoid arthritis: genetic and environmental influences. Expert Rev Clin Immunol 2022, 18, 923-931. https://doi.org/10.1080/1744666X.2022.2106970.
7. Gravallese, E.M.; Firestein, G.S. Rheumatoid Arthritis - Common Origins, Divergent Mechanisms. N Engl J Med 2023, 388(6), 529-542. https://doi.org/10.1056/NEJMra2103726.
8. Finckh, A.; Gilbert, B.; Hodkinson, B.; Bae, S.C.; Thomas, R.; Deane, K.D.; et al. Global epidemiology of rheumatoid arthritis. Nat Rev Rheumatol 2022, 18(9), 591-602. https://doi.org/10.1038/s41584-022-00827-y.
9. Annaji, M.; Mita, N.; Heard, J.; Kang, X.; Poudel, I.; Boddu, S.H.S.; et al. Long-Acting Drug Delivery Technologies for Meloxicam as a Pain Medicine. Crit Rev Ther Drug Carrier Syst 2024, 41(5), 111-150. https://doi.org/10.1615/CritRevTherDrugCarrierSyst.2024048988.
10. Zhang, J.; Froelich, A.; Michniak-Kohn, B. Topical Delivery of Meloxicam using Liposome and Microemulsion Formulation Approaches. Pharmaceutics 2020, 12(3), 282. https://doi.org/10.3390/pharmaceutics12030282.
11. Al-Ameri, A.A.F.; Al-Gawhari, F.J. Formulation Development of Meloxicam Binary Ethosomal Hydrogel for Topical Delivery: In Vitro and In Vivo Assessment. Pharmaceutics 2024, 16(7), 898. https://doi.org/10.3390/pharmaceutics16070898.
12. Nogaeva, U.V.; Leshkevich, A.A.; Yurochkin, D.S.; Golant, Z.M.; Flisyuk, E.V.; Ivkin, D.Y. Prospects of a Transdermal Dosage Form (Microneedles) and Justification of the Active Substance Selection for Development of a New Medicine. Pharm Chem J 2022, 55(9), 1085-1095. https://doi.org/10.1007/s11094-021-02541-7.
13. Zhang, Z.J.; Osmałek, T.; Michniak-Kohn, B. Deformable Liposomal Hydrogel for Dermal and Transdermal Delivery of Meloxicam. Int J Nanomedicine 2020, 15, 9319-9335. https://doi.org/10.2147/IJN.S274954.
14. Dahma, Z.; Torrado-Salmerón, C.; Álvarez-Álvarez, C.; Guarnizo-Herrero, V.; Martínez-Alonso, B.; Torrado, G.; et al. Topical Meloxicam Hydroxypropyl Guar Hydrogels Based on Low-Substituted Hydroxypropyl Cellulose Solid Dispersions. Gels 2024, 10(3), 207. https://doi.org/10.3390/gels10030207.
15. Zhang, Z.J.; Michniak-Kohn, B. Flavosomes, novel deformable liposomes for the co-delivery of anti-inflammatory compounds to skin. Int J Pharm 2020, 585, 119500. https://doi.org/10.1016/j.ijpharm.2020.119500.

16. Rajni; Shah, K.; Dewangan, H.K. Delivery of nano-emulgel carrier: optimization, evaluation and in vivo anti-inflammation estimations for osteoarthritis. Ther Deliv 2024, 15(3), 181-192. https://doi.org/10.4155/tde-2023-0109.
17. Siddiqui, B.; Rehman, A.U.; Haq, I.U.; Ahmad, N.M.; Ahmed, N. Development, optimisation, and evaluation of nanoencapsulated diacerein emulgel for potential use in osteoarthritis. J Microencapsul 2020, 37(8), 595-608. https://doi.org/10.1080/02652048.2020.1829140.
18. Alhasso, B.; Ghori, M.U.; Rout, S.P.; Conway, B.R. Development of a Nanoemulgel for the Topical Application of Mupirocin. Pharmaceutics 2023, 15(9), 2387. https://doi.org/10.3390/pharmaceutics15102387.
19. Alam, M.S.; Algahtani, M.S.; Ahmad, J.; Kohli, K.; Shafiq-Un-Nabi, S.; Warsi, M.H.; et al. Formulation design and evaluation of aceclofenac nanogel for topical application. Ther Deliv 2020, 11(11), 767-778. https://doi.org/10.4155/tde-2020-0076.
20. Ma, Q.; Zhang, J.; Lu, B.; Lin, H.; Sarkar, R.; Wu, T.; et al. Nanoemulgel for Improved Topical Delivery of Desonide: Formulation Design and Characterization. AAPS PharmSciTech 2021, 22(5), 163. https://doi.org/10.1208/s12249-021-02035-5.
21. Bhardwaj, S.; Gaur, P.K.; Tiwari, A. Development of Topical Nanoemulgel Using Combined Therapy for Treating Psoriasis. Assay Drug Dev Technol 2022, 20(1), 42-54. https://doi.org/10.1089/adt.2021.112.
22. Kataria, S.; Roy, S.; Chaurasia, M.; Awasthi, H.; Fatima, Z.; Prasad, R.; et al. Crisaborole loaded nanoemulgel for the mitigation of atopic dermatitis in mice model. Drug Dev Ind Pharm 2023, 49(8), 521-535. https://doi.org/10.1080/03639045.2023.2244075.
23. Siddiqui, A.; Jain, P.; Alex, T.S.; Ali, M.A.; Hassan, N.; Haneef, J.; et al. Investigation of a Minocycline-Loaded Nanoemulgel for the Treatment of Acne Rosacea. Pharmaceutics 2022, 14(10), 2322. https://doi.org/10.3390/pharmaceutics14112322.
24. Algahtani, M.S.; Ahmad, M.Z.; Shaikh, I.A.; Abdel-Wahab, B.A.; Nourein, I.H.; Ahmad, J. Thymoquinone Loaded Topical Nanoemulgel for Wound Healing: Formulation Design and In-Vivo Evaluation. Molecules 2021, 26(12), 3863. https://doi.org/10.3390/molecules26133863.
25. Morsy, M.A.; Abdel-Latif, R.G.; Nair, A.B.; Venugopala, K.N.; Ahmed, A.F.; Elsewedy, H.S.; et al. Preparation and Evaluation of Atorvastatin-Loaded Nanoemulgel on Wound-Healing Efficacy. Pharmaceutics 2019, 11(10), 609. https://doi.org/10.3390/pharmaceutics11110609.
26. Bhardwaj, S.; Bhatia, S.; Gupta, P.S.; Singh, S. Thiazole derivative based topical nanoemulgel for inhibition of bacterial virulence in surface infections. Iran J Basic Med Sci 2022, 25(3), 352-363. https://doi.org/10.22038/IJBMS.2022.59419.13192.
27. Phagna, M.; Badhwar, R.; Singh, M.; Alhalmi, A.; Khan, R.; Noman, O.M.; et al. Development and Characterization of Terbinafine-Loaded Nanoemulgel for Effective Management of Dermatophytosis. Gels 2023, 9(10), 894. https://doi.org/10.3390/gels9110894.
28. Gupta, N.; Gupta, G.D.; Razdan, K.; Albekairi, N.A.; Alshammari, A.; Singh, D. Development of nanoemulgel of 5-Fluorouracil for skin melanoma using glycyrrhizin as a penetration enhancer. Saudi Pharm J 2024, 32(4), 101999. https://doi.org/10.1016/j.jsps.2024.101999.
29. Singh, H.; Bashir, S.M.; Purohit, S.D.; Bhaskar, R.; Rather, M.A.; Ali, S.I.; et al. Nanoceria laden decellularized extracellular matrix-based curcumin releasing nanoemulgel system for full-thickness wound healing. Biomater Adv 2022, 137, 212806. https://doi.org/10.1016/j.bioadv.2022.212806.

30. Al Fatease, A.; Alqahtani, A.; Khan, B.A.; Mohamed, J.M.M.; Farhana, S.A. Preparation and characterization of a curcumin nanoemulsion gel for the effective treatment of mycoses. Sci Rep 2023, 13(1), 22730. https://doi.org/10.1038/s41598-023-49328-2.
31. Alhasso, B.; Ghori, M.U.; Conway, B.R. Development of Nanoemulsions for Topical Application of Mupirocin. Pharmaceutics 2023, 15(2), 378. https://doi.org/10.3390/pharmaceutics15020378.
32. Nawaz, A.; Latif, M.S.; Alnuwaiser, M.A.; Ullah, S.; Iqbal, M.; Alfatama, M.; et al. Synthesis and Characterization of Chitosan-Decorated Nanoemulsion Gel of 5-Fluorouracil for Topical Delivery. Gels 2022, 8(7), 412. https://doi.org/10.3390/gels8070412.
33. Indrati, O.; Martien, R.; Rohman, A.; Nugroho, A.K. Development of Nanoemulsion-based Hydrogel Containing Andrographolide: Physical Properties and Stability Evaluation. J Pharm Bioallied Sci 2020, 12(Suppl 2), S816-S820. https://doi.org/10.4103/jpbs.JPBS_174_20.
34. Khan, R.U.; Shah, S.U.; Rashid, S.A.; Naseem, F.; Shah, K.U.; Farid, A.; et al. Lornoxicam-Loaded Chitosan-Decorated Nanoemulsion: Preparation and In Vitro Evaluation for Enhanced Transdermal Delivery. Polymers (Basel) 2022, 14, 1922. https://doi.org/10.3390/polym14091922.
35. Zhang, Y.; Gao, Z.; Chao, S.; Lu, W.; Zhang, P. Transdermal delivery of inflammatory factors regulated drugs for rheumatoid arthritis. Drug Deliv 2022, 29(1), 1934-1950. https://doi.org/10.1080/10717544.2022.2089295.
36. Sithole, M.N.; Marais, S.; Maree, S.M.; Du Plessis, L.H.; Du Plessis, J.; Gerber, M. Development and characterization of nano-emulsions and nano-emulgels for transdermal delivery of statins. Expert Opin Drug Deliv 2021, 18(6), 789-801. https://doi.org/10.1080/17425247.2021.1867533.
37. Yang, M.; Yang, D.; Han, L.; Fan, Z.; Liu, J.; Yuan, Y. Triptolide Nanoemulsion Gel as a Transdermal Drug Delivery System: Preparation, Pharmacokinetics, and Rheumatoid Arthritis Evaluation. Curr Drug Deliv 2025. https://doi.org/10.2174/1567201821666230808114519.
38. Wang, Y.; Zhang, Q.; Wei, Y.; Cai, X.; Li, Z.; Wu, Q.; et al. Retinol semisolid preparations in cosmetics: transcutaneous permeation mechanism and behaviour. Sci Rep 2024, 14(1), 22793. https://doi.org/10.1038/s41598-024-73240-y.
39. Saab, M.; Raafat, K.; El-Maradny, H. Transdermal Delivery of Capsaicin Nanoemulgel: Optimization, Skin Permeation and In Vivo Activity against Diabetic Neuropathy. Adv Pharm Bull 2022, 12(4), 780-790. https://doi.org/10.34172/apb.2022.080.
40. Miranda, M.; Pais, A.A.C.C.; Cardoso, C.; Vitorino, C. aQbD as a platform for IVRT method development - A regulatory oriented approach. Int J Pharm 2019, 572, 118695. https://doi.org/10.1016/j.ijpharm.2019.118695.